LUND UNIVERSITY

Single GaInP nanowire p-i-n junctions near the direct to indirect bandgap crossover point

Wallentin, Jesper; Poncela, Laura Barrutia; Jansson, Anna M.; Mergenthaler, Kilian; Ek, Martin; Jacobsson, Daniel; Wallenberg, Reine; Deppert, Knut; Samuelson, Lars; Hessman, Dan; Borgström, Magnus

Link to publication

Related Articles

Valence band offset of n-ZnO/p-MgxNi1−xO heterojunction measured by x-ray photoelectron spectroscopy
Appl. Phys. Lett. 101, 052109 (2012)

Diamond/aluminium nitride composites for efficient thermal management applications
Appl. Phys. Lett. 101, 051902 (2012)

Illumination effects on electrical characteristics of GaN/AlGaN/GaN heterostructures and heterostructure field effect transistors and their elimination by proper surface passivation
J. Appl. Phys. 112, 014511 (2012)

Hole transport in pure and doped hematite
J. Appl. Phys. 112, 013701 (2012)

AlSb nucleation induced anisotropic electron mobility in AlSb/InAs heterostructures on GaAs
Appl. Phys. Lett. 100, 262103 (2012)

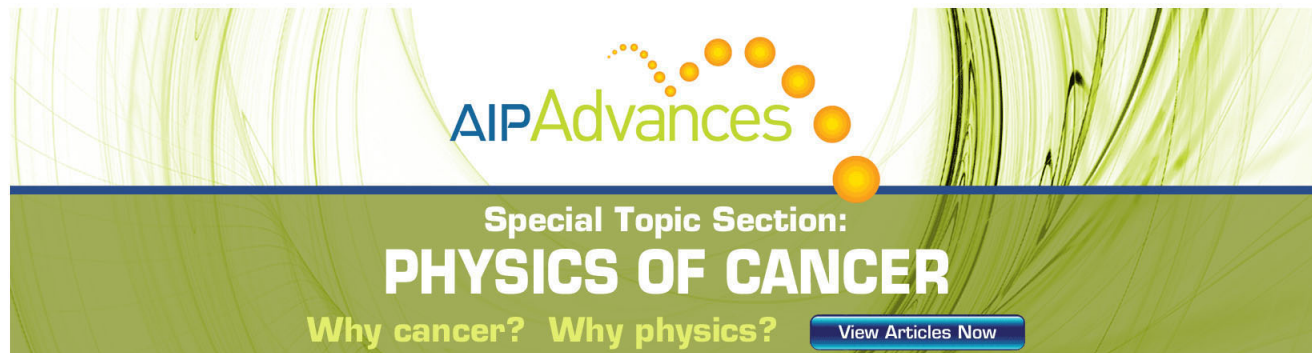## Additional information on Appl. Phys. Lett.

Journal Homepage: http://apl.aip.org/

Journal Information: http://apl.aip.org/about/about_the_journal

Top downloads: http://apl.aip.org/features/most_downloaded

Information for Authors: http://apl.aip.org/authors

Single GaInP nanowire p-i-n junctions near the direct to indirect bandgap crossover point

Jesper Wallentin,[1,a] Laura Barrutia Poncela,[1] Anna M. Jansson,[1] Kilian Mergenthaler,[1] Martin Ek,[2] Daniel Jacobsson,[1] L. Reine Wallenberg,[2] Knut Deppert,[1] Lars Samuelson,[1] Dan Hessman,[1] and Magnus T. Borgström[1]

[1]Solid State Physics, Lund University, Box 118, S-221 00, Lund, Sweden
[2]Polymer & Materials Chemistry/nCHREM, Lund University, Box 124, S-221 00, Lund, Sweden

Axially defined GaInP single nanowire (NW) p-i-n junctions are demonstrated, with photocurrent response and yellow-green electroluminescence near the indirect bandgap crossover point at 2.18 eV (569 nm). We use DEZn and H_2S as p- and n-type dopants, and find that they both affect the material composition and the crystal structure. The photovoltaic efficiency is comparable to single NW devices from binary III-V materials. These results demonstrate the potential of GaInP nanowires as a high-bandgap material for multijunction solar cells and light-emitting devices in the visible regime. © 2012 American Institute of Physics. [http://dx.doi.org/10.1063/1.4729929]

Semiconductor III-V nanowires (NWs) are promising components for optoelectronic devices such as light emitting diodes (LEDs)[1,2] and photovoltaics.[3–6] The ternary compound $Ga_xIn_{1-x}P$, for simplicity hereafter referred to as GaInP (InGaP), is a standard part of multijunction solar cells, since it can be grown with a bandgap of around 1.9 eV when lattice-matched to GaAs or Ge.[7] GaInP shells grown on GaAs NW cores have been used for NW-based LEDs on silicon,[8] while others have investigated strained GaInP NW shells[9,34] and molecular beam epitaxy (MBE)-grown GaInP NWs.[10]

Theoretically, GaInP can reach a direct band gap of up to about 2.2 eV at room temperature,[11] but at the corresponding composition there is no suitable substrate for thin-film growth. Axial NW heterostructures, however, can be grown with large lattice mismatch since the strain can be relaxed vertically, and here we demonstrate devices with a bandgap close to the theoretical limit. Controlled doping is necessary for most applications,[12] and here we use DEZn and H_2S for p- and n-doping of GaInP. We demonstrate axially defined GaInP p-i-n junctions with yellow-green electroluminescence.

We grew Au-seeded GaInP NWs on InP (111)B substrates in metal organic vapor phase epitaxy (MOVPE), starting from an InP NW stub and using a GaP barrier for improved photoluminescence (PL). The yield of vertical NWs was close to 100%. In this work, we focus on doped GaInP NWs, while a growth parameter study of undoped GaInP NWs has been reported separately.[13] Hydrogen chloride (HCl) was used to control the radial growth.[13,14] NWs were made non-intentionally doped ("undoped"), using H_2S for n-doping, using DEZn for p-doping, and finally with an axially defined p-i-n doped structure. See supplementary material for methods details.[15]

Doping using H_2S did not affect the growth rate, similarly to InP NWs grown with HCl,[16] while DEZn lowered the growth rate by around 65%. Slightly lowered growth rates have previously been observed in DEZn-doped InP NWs.[17]

Transmission electron microscopy (TEM) of the p-i-n NWs revealed that the undoped segment had the zincblende crystal structure with rotational twins and some short wurtzite segments. The Zn-doped segment had longer segments of pure zinc blende and more regular twinning, which is expected since both InP (Refs. 18 and 19) and GaP (Ref. 20) NWs form zinc blende with regular twinning when doped with Zn. The S-doped segment was almost pure wurtzite, similar to S-doped InP NWs.[21]

We investigated the effect of doping on the composition of the ternary $Ga_xIn_{1-x}P$ NWs using energy dispersive x-ray spectroscopy (EDS) line scans along the length of p-i-n doped NWs, shown in Fig. 1(a). The undoped segment showed an average composition of around $x = 0.77$ (standard deviation 0.05). The line scan indicated a slightly decreasing Ga concentration along the NW.

The S-doped segment was a bit more In-rich, with $x = 0.70$, and showed a slightly decreasing Ga concentration in the growth direction. Possibly, the change in crystal structure affected the group III diffusion lengths in favor of In.

The effect from DEZn was more complicated, creating first a segment with lower Ga content, $x = 0.63$, which then gradually increased up to about $x = 0.85$. Zn has a high solubility in liquid metals, and we speculate that Zn affects the equilibrium composition of the seed particle to low Ga levels when it is introduced. Note that the use of DEZn lowered the growth rate significantly. We speculate that DEZn decreases the diffusion length of In precursors, as previously observed for InP NWs,[17] thereby gradually increasing the Ga concentration.

The optical properties were investigated using single NW PL at low temperature (4.2 K), shown in Fig. 1(b), and macro-PL at room temperature of the as-grown NWs. For these measurements, homogenously doped GaInP NWs were investigated, grown under the same respective conditions as in the combined p-i-n structure. The non-intentionally doped NWs showed a low temperature PL signal in the range 1.95 to 2.3 eV, with many relatively sharp peaks, as well as room temperature macro-PL displaying one relatively broad peak centered at 2.14 eV. The average composition, $x = 0.77$, is
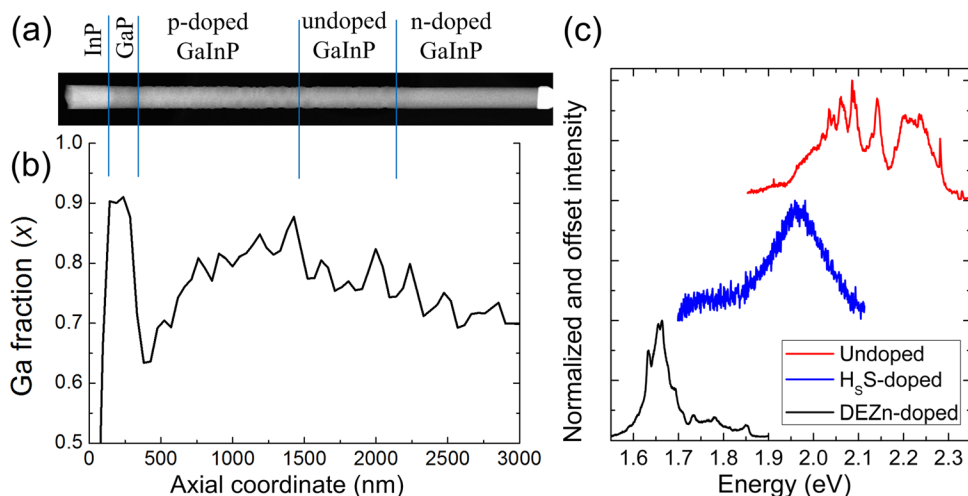
a)Electronic mail: jesper.wallentin@ftf.lth.se.

FIG. 1. (a) High angle annular dark field (HAADF) image of p-i-n doped GaInP NW. (b) Ga fraction, x, calculated from an EDS line scan and point analysis. The growth direction in (a) and (b) is to the right. (c) Low-temperature (4.2 K) photoluminescence from undoped and homogenously doped single GaInP NWs. The spectra have been offset and normalized for clarity.

slightly above the predicted direct to indirect crossover,[11] and the highest PL signal at about 2.25 eV fits well with the predicted crossover bandgap at low temperature. The lower-energy peaks at low temperature could be related to the observed stacking faults,[22] or possibly surface-related states.[23] Ordering is another possible explanation for the relatively low-energy PL,[24] but synchrotron-based x-ray diffraction measurements do not show any signs of this.[13] There may also be In-rich segments, which could be shorter than the resolution in EDS (about 5 nm), and could occur both axially, radially, as observed in GaInN NWs,[25] or at the NW edges as observed in AlInP NW shells.[26] Note, however, that we did not observe radial growth of a Ga-rich shell in TEM,[13] as previously found in MBE-grown GaInP.[10] At room temperature, the carriers recombine before diffusing to these low-bandgap regions, thereby explaining the observed single peak.

The S-doped NWs showed low-T PL with one broad peak around 1.95 eV, while the Zn-doped NWs showed one main peak at 1.65 eV and several weaker peaks. Similar to the low-energy peaks in the undoped NWs, both types of doping thus resulted in PL about 0.4 eV below the bandgap as expected from the composition measured with EDS. We speculate that similar effects as in the undoped NWs, i.e., short In-rich segments, are responsible for the discrepancy. In the Zn-doped NWs, there could also be significant redshift from Fermi level pinning at the surface[27] and acceptor states.[28]

Regarding the S-doped NWs, the spectrum shows qualitative similarity with highly S-doped InP NWs.[21] Electrical measurements (see below) indicate quite high doping levels. We speculate that the high electron concentration leads to state-filling, causing the In-rich regions to be filled with electrons up to a common Fermi level. This would explain the lack of distinct peaks as in the undoped material.

For electrical characterization of homogenously doped NWs, we created NW-FETs.[29] S-doped devices showed linear source-drain behavior with resistances of around 10 MΩ, several orders of magnitude higher than InP NWs grown with similar HCl and H_2S molar fractions.[16] See supplementary material for details.[15] The current increased with a positive gate which demonstrated n-type conductance, but the mobility as calculated from the transconductance in

gate-sweep measurements gave an unreasonably low value of around 10^{-2} cm²/Vs. We believe that the contacts, despite showing ohmic behavior, dominated the device resistance rather than the NW themselves.

Zn-doped NW-FETs showed non-linear I-V characteristics, indicating Schottky-like barriers at the contacts. The currents were significantly higher than in Zn-doped InP NW-FETs,[4] which demonstrates better contacts but not necessarily higher doping of the NWs. The gate-sweep measurements showed weak gate dependence but clear p-type behavior.

Having demonstrated p- and n-doping, we synthesized p-i-n doped devices. Dark I-V measurements, shown in Fig. 2(a), displayed clear rectification with typical diode behavior. The ideality factor, n, was around 2.1 at low bias, which is slightly higher than similar InP (Ref. 4) and GaAs (Ref. 30) devices. The rectifying behavior demonstrates that HCl prevents the overgrowth of a conductive n-type shell.

The photocurrents were on the same order of magnitude as single NW InP p-n junctions.[4] A proper solar cell efficiency could not be calculated since we used a laser for excitation, and since the absorption in nanowires is difficult to evaluate. However, using a simple analysis with a projected absorption area equal to the i-region, we achieve similar efficiencies as previously published single-NW devices.[6,30] We plotted the short-circuit current vs. laser power (Fig. 2(b)) and found a linear dependence over five orders of magnitude. The open-circuit voltage V_{oc} should depend on the power as $V_{oc} = (nkT/q)\ln(I_L/I_0)$.[31] Here, I_L is the light-induced current, which was proportional to the laser intensity, and I_0 the dark current. In good agreement with this model, we found a logarithmic dependence of V_{oc} on the excitation power, with a slope of 53 mV. Assuming $kT/q = 26$ mV, this gives an ideality factor of 2.04 in close agreement with the dark I-V measurements. The fill factor at the highest excitation was 43%, and was almost independent of laser power.

Next, we investigated the spectral dependence of the photocurrent, shown in Fig. 2(c). The device showed a quite sharp onset around 2.15 eV, in good agreement with the room-T PL and sharper than the broad peak observed in low-T PL. This indicates that the many small peaks observed in low-T PL are indeed related to small narrow-bandgap regions. Also surprising is the plateau in photocurrent above 2.25 eV. This effect could be related to the indirect X and L
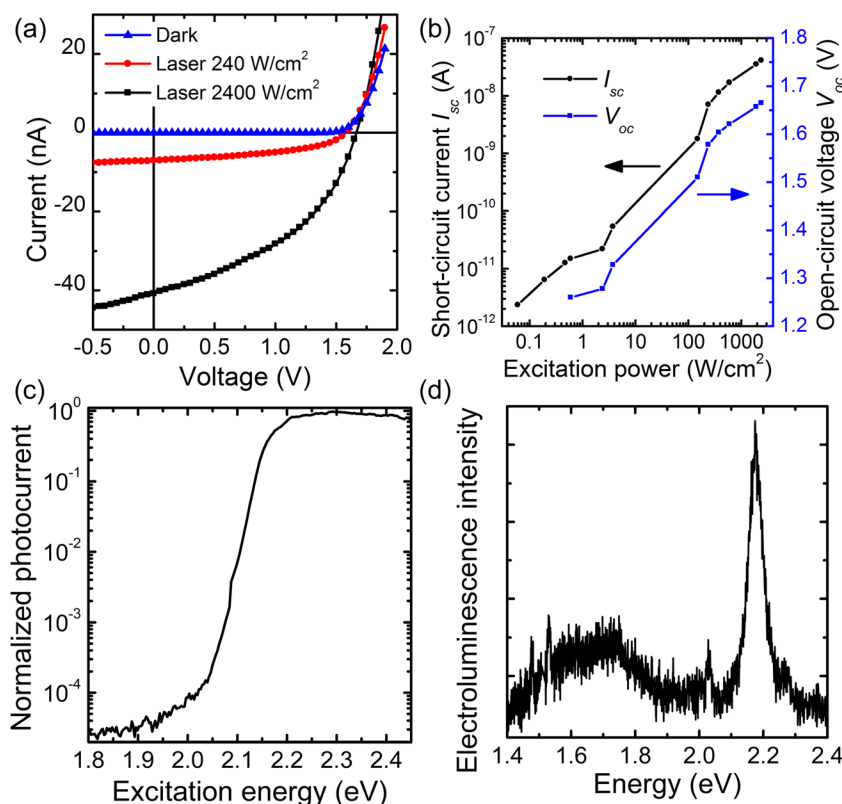
FIG. 2. Optoelectrical characterization of a single NW GaInP p-i-n junction: (a) I-V, dark and illuminated by a 532 nm laser. (b) Excitation power dependence of short-circuit current and open-circuit voltage. (c) Photocurrent as a function of the excitation energy, normalized to the source spectral intensity (d) Electroluminescence spectrum under 2.3 V forward bias.

bands, which both have minima of around 2.2–2.3 eV at this composition.[11] Absorption should be effective in these bands due to the high effective masses, where possibly carriers get trapped without contributing to the photocurrent. However, the saturation could also be an optical effect due to reduced coupling of short wavelength light into the NWs.[32]

Finally, we investigated the electroluminescence spectrum under forward bias, i.e., in LED mode, shown in Fig. 2(d). The spectrum shows two peaks. The high-energy peak at 2.18 eV is in good agreement with the photocurrent spectroscopy and the room-T PL, and is presumably due to recombination in the undoped region. Note that this peak has a wavelength of about 569 nm, i.e., yellow-green. There is a second, broader peak around 1.5 to 1.8 eV, which we attribute to recombination in the lower-bandgap doped regions.

The quantum efficiency was only around 4×10^{-8}, which is very low even for a NW p-n junction and several orders of magnitude less than single NW InP LEDs.[33] With the measured variations in composition, the band structure shows a high-bandgap i-region surrounded by lower-bandgap p- and n-segments. Thus, carriers will tend to escape the i-region which enhances carrier separation rather than recombination. It is therefore not surprising that the GaInP p-i-n junctions showed good photocurrent characteristics but poor LED efficiency. It should be possible to achieve a more beneficial band structure for LEDs, by tuning the TMG to TMI ratio during growth to create a low-bandgap i-region.

In conclusion, we have demonstrated p- and n-doping of GaInP NWs. Both types of doping affected the bandgap and crystal structure, but in different ways. The efficient PL and photovoltaic effect, despite the stacking faults and lack of a high-bandgap shell, indicates a low density of non-radiative traps. The p-i-n doped devices show good photocurrent

behavior but poor LED efficiency, attributed to the high-bandgap middle segment. These results demonstrate that GaInP NW optoelectronic devices can be made with bandgaps significantly exceeding the composition range available in thin films.

[1]X. F. Duan, Y. Huang, Y. Cui, J. F. Wang, and C. M. Lieber, Nature (London) **409**(6816), 66 (2001).
[2]E. D. Minot, F. Kelkensberg, M. van Kouwen, J. A. van Dam, L. P. Kouwenhoven, V. Zwiller, M. T. Borgström, O. Wunnicke, M. A. Verheijen, and E. P. A. M. Bakkers, Nano Lett. **7**(2), 367 (2007).
[3]K. N. Hajime Goto, K. Tomioka, S. Hara, and J. M. Kenji Hiruma, and T. Fukui, Appl. Phys. Express **2**(2009), 035004 (2009).
[4]M. T. Borgström, J. Wallentin, M. Heurlin, S. Fält, P. Wickert, J. Leene, M. H. Magnusson, K. Deppert, and L. Samuelson, IEEE J. Sel. Top. Quantum Electron. **17**(4), 1050 (2011).
[5]B. Tian, T. J. Kempa, and C. M. Lieber, Chem. Soc. Rev. **38**(1), 16 (2009).
[6]C. Colombo, M. Heibeta, M. Gratzel, and A. Fontcuberta i Morral, Appl. Phys. Lett. **94**(17), 173108 (2009).
[7]R. R. King, D. C. Law, K. M. Edmondson, C. M. Fetzer, G. S. Kinsey, H. Yoon, R. A. Sherif, and N. H. Karam, Appl. Phys. Lett. **90**(18), 183516 (2007).
[8]C. P. T. Svensson, T. Mårtensson, J. Trägårdh, C. Larsson, M. Rask, D. Hessman, L. Samuelson, and J. Ohlsson, Nanotechnology **19**(30), 305201 (2008).
[9]N. Sköld, L. S. Karlsson, M. W. Larsson, M. E. Pistol, W. Seifert, J. Trägårdh, and L. Samuelson, Nano Lett. **5**(10), 1943 (2005).
[10]A. Fakhr, Y. M. Haddara, and R. R. LaPierre, Nanotechnology **21**(16), 165601 (2010).
[11]J. W. Nicklas and J. W. Wilkins, Appl. Phys. Lett. **97**(9), 091902 (2010).

[12]J. Wallentin and M. T. Borgström, J. Mater. Res. **26**(17), 2142 (2011).
[13]D. Jacobsson, J. M. Persson, D. Kriegner, T. Etzelstorfer, J. Wallentin, J. B. Wagner, J. Stangl, L. Samuelson, K. Deppert, and M. T. Borgström, Nanotechnology **23**, 245601 (2011).
[14]M. T. Borgström, J. Wallentin, J. Trägårdh, P. Ramvall, M. Ek, L. R. Wallenberg, L. Samuelson, and K. Deppert, Nano Res. **3**(4), 264 (2010).
[15]See supplementary material at http://dx.doi.org/10.1063/1.4729929 for methods details and electrical measurements of homogenously doped NWs.
[16]J. Wallentin, M. Ek, L. R. Wallenberg, L. Samuelson, and M. T. Borgström, Nano Lett. **12**(1), 151 (2011).
[17]J. Wallentin, P. Wickert, M. Ek, A. Gustafsson, L. R. Wallenberg, M. H. Magnusson, L. Samuelson, K. Deppert, and M. T. Borgstrom, Appl. Phys. Lett. **99**(25), 253105 (2011).
[18]R. E. Algra, M. A. Verheijen, M. T. Borgström, L.-F. Feiner, G. Immink, W. J. P. van Enckevort, E. Vlieg, and E. P. A. M. Bakkers, Nature (London) **456**(7220), 369 (2008).
[19]J. Wallentin, M. Ek, L. R. Wallenberg, L. Samuelson, K. Deppert, and M. T. Borgström, Nano Lett. **10**(12), 4807 (2010).
[20]R. E. Algra, M. A. Verheijen, L.-F. Feiner, G. G. W. Immink, W. J. P. v. Enckevort, E. Vlieg, and E. P. A. M. Bakkers, Nano Lett. **11**(3), 1259 (2011).
[21]J. Wallentin, K. Mergenthaler, M. Ek, L. R. Wallenberg, L. Samuelson, K. Deppert, M. E. Pistol, and M. T. Borgström, Nano Lett. **11**(6), 2286 (2011).
[22]J. M. Bao, D. C. Bell, F. Capasso, J. B. Wagner, T. Mårtensson, J. Trägårdh, and L. Samuelson, Nano Lett. **8**(3), 836 (2008).
[23]I. Shalish, H. Temkin, and V. Narayanamurti, Phys. Rev. B **69** 24), 245401 (2004).
[24]T. Suzuki, A. Gomyo, and S. Iijima, J. Cryst. Growth **93**(1–4), 396 (1988).
[25]G. Tourbot, C. Bougerol, A. Grenier, M. Den Hertog, D. Sam-Giao, D. Cooper, P. Gilet, B. Gayral, and B. Daudin, Nanotechnology **22**(7), 075601 (2011).
[26]N. Sköld, J. B. Wagner, G. Karlsson, T. Hernan, W. Seifert, M. E. Pistol, and L. Samuelson, Nano Lett **6**(12), 2743 (2006).
[27]M. H. M. van Weert, O. Wunnicke, A. L. Roest, T. J. Eijkemans, A. Yu Silov, J. E. M. Haverkort, G. W. 't Hooft, and E. P. A. M. Bakkers, Appl. Phys. Lett. **88**(4), 043109 (2006).
[28]Y. Moon, S. Si, E. Yoon, and S. J. Kim, J. Appl. Phys. **83**(4), 2261 (1998).
[29]Y. Cui, X. F. Duan, J. T. Hu, and C. M. Lieber, J. Phys. Chem. B **104**(22), 5213 (2000).
[30]A. Lysov, S. Vinaji, M. Offer, C. Gutsche, I. Regolin, W. Mertin, M. Geller, W. Prost, G. Bacher, and F.-J. Tegude, Nano Res. **4**(10), 987 (2011).
[31]S. Sze, *Physics of Semiconductor Devices* (Wiley, New York, 1981).
[32]L. Y. Cao, J. S. White, J. S. Park, J. A. Schuller, B. M. Clemens, and M. L. Brongersma, Nature Mater. **8**(8), 643 (2009).
[33]M. T. Borgström, E. Norberg, P. Wickert, H. A. Nilsson, J. Trägårdh, K. A. Dick, G. Statkute, P. Ramvall, K. Deppert, and L. Samuelson, Nanotechnology **19**(44), 445602 (2008).
[34]J. Tatebayashi, A. Lin, P. S. Wong, R. F. Hick, and D. L. Huffaker, J. Appl. Phys. **108**(3), 034315 (2010).